Recent advances in quasi-2D superconductors viaorganic molecule intercalation

Mengzhu Shi(石孟竹), Baolei Kang(康宝蕾), Tao Wu(吴涛), and Xianhui Chen(陈仙辉)
Citation: Chin. Phys. B, 2022, 31 (**10**): 107403. DOI: 10.1088/1674-1056/ac8e9d
Journal homepage: http://cpb.iphy.ac.cn; http://iopscience.iop.org/cpb

What follows is a list of articles you may be interested in

Superconductivity and unconventional density waves in vanadium-based kagome materials AV_3Sb_5

Hui Chen(陈辉), Bin Hu(胡彬), Yuhan Ye(耶郁晗), Haitao Yang(杨海涛), and Hong-Jun Gao(高鸿钧)
Chin. Phys. B, 2022, 31 (**9**): 097405. DOI: 10.1088/1674-1056/ac7f95

Josephson vortices and intrinsic Josephson junctions in the layered iron-based superconductor $Ca_{10}(Pt_3As_8)((Fe_{0.9}Pt_{0.1})_2As_2)_5$

Qiang-Tao Sui(随强涛) and Xiang-Gang Qui(邱祥冈)
Chin. Phys. B, 2022, 31 (**9**): 097403. DOI: 10.1088/1674-1056/ac76ae

Superconductivity in $CuIr_{2-x}Al_xTe_4$ telluride chalcogenides

Dong Yan(严冬), Lingyong Zeng(曾令勇), Yijie Zeng(曾宜杰), Yishi Lin(林一石), Junjie Yin(殷俊杰), Meng Wang(王猛), Yihua Wang(王熠华), Daoxin Yao(姚道新), and Huixia Luo(罗惠霞)
Chin. Phys. B, 2022, 31 (**3**): 037406. DOI: 10.1088/1674-1056/ac43b1

Electrical and thermoelectric study of two-dimensional crystal of $NbSe_2$

Xin-Qi Li(李新祺), Zhi-Lin Li(李治林), Jia-Ji Zhao(赵嘉佶), Xiao-Song Wu(吴孝松)
Chin. Phys. B, 2020, 29 (**8**): 087402. DOI: 10.1088/1674-1056/ab9614

Direct evidence of high temperature superconductivity in one-unit-cell FeSe films on $SrTiO_3$ substrate by transport and magnetization measurements

Xing Ying, Wang Jian
Chin. Phys. B, 2015, 24 (**11**): 117404. DOI: 10.1088/1674-1056/24/11/117404

TOPICAL REVIEW — Celebrating 30 Years of *Chinese Physics B*

Recent advances in quasi-2D superconductors via organic molecule intercalation

Mengzhu Shi(石孟竹)[1,2], Baolei Kang(康宝蕾)[1,2], Tao Wu(吴涛)[1,2], and Xianhui Chen(陈仙辉)[1,2,3,4,†]

[1] *Department of Physics, University of Science and Technology of China, Hefei* 230026, *China*
[2] *CAS Key Laboratory of Strongly-coupled Quantum Matter Physics, University of Science and Technology of China, Hefei* 230026, *China*
[3] *Collaborative Innovation Center of Advanced Microstructures, Nanjing University, Nanjing* 210093, *China*
[4] *CAS Center for Excellence in Superconducting Electronics (CENSE), Shanghai* 200050, *China*

(Received 16 July 2022; revised manuscript received 26 August 2022; accepted manuscript online 2 September 2022)

Superconductivity at the 2D limit shows emergent novel quantum phenomena, including anomalously enhanced H_{c2}, quantum metallic states and quantum Griffiths singularity, which has attracted much attention in the field of condensed matter physics. In this article, we focus on new advances in quasi-2D superconductors in the bulk phase using an organic molecular electrochemical intercalation method. The enhanced superconductivity and emergent pseudogap behavior in these quasi-2D superconductors are summarized with a further prospect.

Keywords: organic molecular intercalation, two-dimensional superconductivity, organic-inorganic hybrid materials

PACS: 74.25.–q, 74.25.F–, 74.70.Xa **DOI:** 10.1088/1674-1056/ac8e9d

1. Introduction

Superconductivity (SC) is a macroscopic quantum phenomenon. Generally, with reduced dimensionality, the increased spatial and temporal fluctuations will strongly suppress and even destroy superconductivity in systems.[1–5] Within classical theories, the famous Mermin–Wagner theorem points out that continuous spontaneous symmetry breaking is forbidden in neither one- nor two-dimensional systems at finite temperatures, thus disenabling conventional superconducting transitions at the 2D limit.[2] Nevertheless, the Berezinskii–Kosterlitz–Thouless (BKT) theory provides a compatible understanding for this issue. It predicts a thermodynamic instability in the form of vortex–antivortex pairs, which spontaneously dissociate into free vortices at a characteristic transition temperature T_{BKT}.[6–8] Such a transition is a topological phase transition without any form of symmetry breaking, which manifests itself as a jump in the power-law exponent in current–voltage (I–V) characteristic curves and in a disappearance of ohmic resistance obeying the Halperin–Nelson scaling law.[9,10] At present, BKT physics has become an important feature of 2D superconductors.

In the past few decades, superconductivity at the 2D limit has become one of the hottest frontiers in the field of condensed matter physics. The emergent novel quantum phenomena, including anomalously enhanced H_{c2}, quantum metallic states and quantum Griffiths singularity in conventional Bardeen–Cooper–Schrieffer (BCS) superconductors, shed light on not only fundamental research but also practical applications to non-dissipative micro/nanoelectronics.[11–16] Particularly, distinct from conventional BCS superconductors, all high-T_c superconductors have a layered structure with varying degrees of anisotropy. Very recently, monolayer $Bi_2Sr_2CaCu_2O_{8+\delta}$ (Bi2212) has been reported to display all the fundamental physics of high-T_c superconductivity as its three-dimensional (3D) counterparts, verifying the quasi-2D nature of its bulk state.[17] Coincidentally, for iron-based superconductors that have a more 3D layered structure, the discovery of exotic high-T_c superconductivity in a single-layer FeSe film on a $SrTiO_3$ substrate (FeSe/STO) further highlights the key role of reduced dimensionality.[18,19] It exhibits a large superconducting gap of approximately 20 meV with a gap opening temperature of approximately 65 K, while the zero-resistance critical temperature (T_{c0}) determined by electrical transport measurements is mostly below 40 K.[20–23] Such a result reveals much enhanced high-T_c superconductivity compared to its 3D bulk phase and possible links with the pseudogap behavior in high-T_c cuprate superconductors.[24–27] The apparent dichotomy with conventional BCS superconductors hints at great importance for the quasi-2D nature of both cuprate and iron-based superconductors, which provides a unique perspective for the experimental study of high-T_c superconductors.

In the early days, the most popular methods for the fabrication of 2D superconductors were thermal evaporation and sputtering of granular and amorphous metallic film.[28,29] Driven by the rapid advancement in film growth techniques,

†Corresponding author. E-mail: chenxh@ustc.edu.cn

including molecular beam epitaxy (MBE) and pulsed laser deposition (PLD), the existence of 2D superconductors with truly atomic-scale thickness and the fabrication of complicated heterostructures have been established.[15,30,31] In addition to the bottom-up approaches that start from the atomic ingredients, mechanical exfoliation and liquid exfoliation provide an alternative to fabricate 2D superconductors through up-bottom approaches.[32–34] However, restricted by the limited size and intrinsic features of thin films, intensive studies in the traditional experimental framework based on bulk samples, such as specific heat, anisotropic electrical transport and NMR measurements, have been totally impeded. Here, we explore a series of quasi-2D superconductors in bulk phase, which are synthesized through a simple and gentle method, that is, electrochemical intercalation.[35–38] New advances in these quasi-2D superconductors in the bulk phase are the focus of this review article. Our results establish dimensionality as an effective parameter for studying novel physics in both BCS superconductors and high-T_c superconductors.

2. Experimental techniques

There are several methods to achieve or enhance the two-dimensionalization in 2D materials with high crystallinity. The first method to enhance the two-dimensionality is to insert inorganic insulating layers with different thicknesses between the functional layers. For example, in the study of cuprate superconductors, T_c can be gradually increased by inserting insulating inorganic layers with different thicknesses into the CuO_2 plane. Taking the Hg-Ba-Ca-Cu-O system as an example, the T_c of the material gradually increases with increasing thickness of the inorganic insulating layer.[39] However, such a series of materials make it difficult to obtain large crystals, and only several limited systems have been reported. The second method to realize two-dimensionalization is to change the thickness of the material by the micromechanical exfoliation method or the growth of thin films through the molecular beam epitaxy (MBE) or chemical vapour deposition (CVD) method. This is a more general way to modify the physical properties of the material by dimensionality control. With decreasing thickness, different types of charge density wave (CDW) orders can be observed, and the magnetic transition temperature or T_c can also be regulated. For example, the TaS_2 thin flake sample shows a thickness-dependent CDW state.[40] With decreasing thickness, the CDW transition temperature of 1T-TaS_2 gradually decreases and finally disappears. The T_c of $NbSe_2$ decreases with decreasing thickness.[41] However, the T_c of single layer FeSe/$SrTiO_3$ as high as 65 K is much higher than that of bulk FeSe,[20–23] which has a low T_c of only approximately 8 K. Despite the many advantages mentioned above, the problem of these thin layer samples is that it is difficult to obtain large enough samples for structural research, specific heat testing, anisotropic resistance, anisotropic susceptibility and NMR measurements.

Recently, a new method for the synthesis of two-dimensional bulk materials has attracted much attention.[35,36] It enables the measurement of the correlated electronic properties of two-dimensional systems with strong anisotropy. That is the organic molecules intercalation method where the organic molecules are inserted into the interlayer of two-dimensional materials.

Intercalation is a widely used method for material preparation. Many ions, molecular and inorganic structural layers can be inserted into the two-dimensional materials, which is very significant in graphite intercalation compounds. Compared with the inserted alkali metals, the insertion of organic molecules can greatly increase the interlayer distance and realize a two-dimensional structure. At the same time, due to the poor conductivity of the organic molecular layer, the transport of electrons can only be confined in the inorganic layer within the *ab* plane, and it is difficult to transmit between layers in the *c*-axis direction, which may lead to the two-dimensional transport characteristics of charges and spin.

In our previous work, we adopted the electrochemical intercalation method to tune the physical properties, especially the superconductivity of 2D materials. Electrochemical intercalation can be easily realized through the driving force of the current. As shown in Fig. 1(a), an electrolytic cell is assembled with the target material as the working electrode, the Ag piece as the counter electrode and the solution containing quaternary ammonium cations as the electrolyte.[42] A constant current is applied to the above electrolytic cell. When the current passes through the cell, the counter electrode loses electrons, and the working electrode obtains electrons accompanied by the insertion of organic ions to maintain the charge balance.

Taking TaS_2 as an example, the above process can be expressed by the following equations:

$$\mathrm{Br^- - e^- + Ag = AgBr},$$
$$\mathrm{TaS_2 + e^- + }x\mathrm{CTA^+ = (CTA)}_x\mathrm{TaS_2}.$$

After cleaning and drying the product, we obtained the organic ion intercalated bulk sample for further physical measurements. Through the above electrochemical intercalation process, we can quickly obtain crystals with an *ab* plane size greater than 1 mm for various bulk measurements, including structure characterization, anisotropic resistance and susceptibility measurements, specific heat tests and NMR measurements.

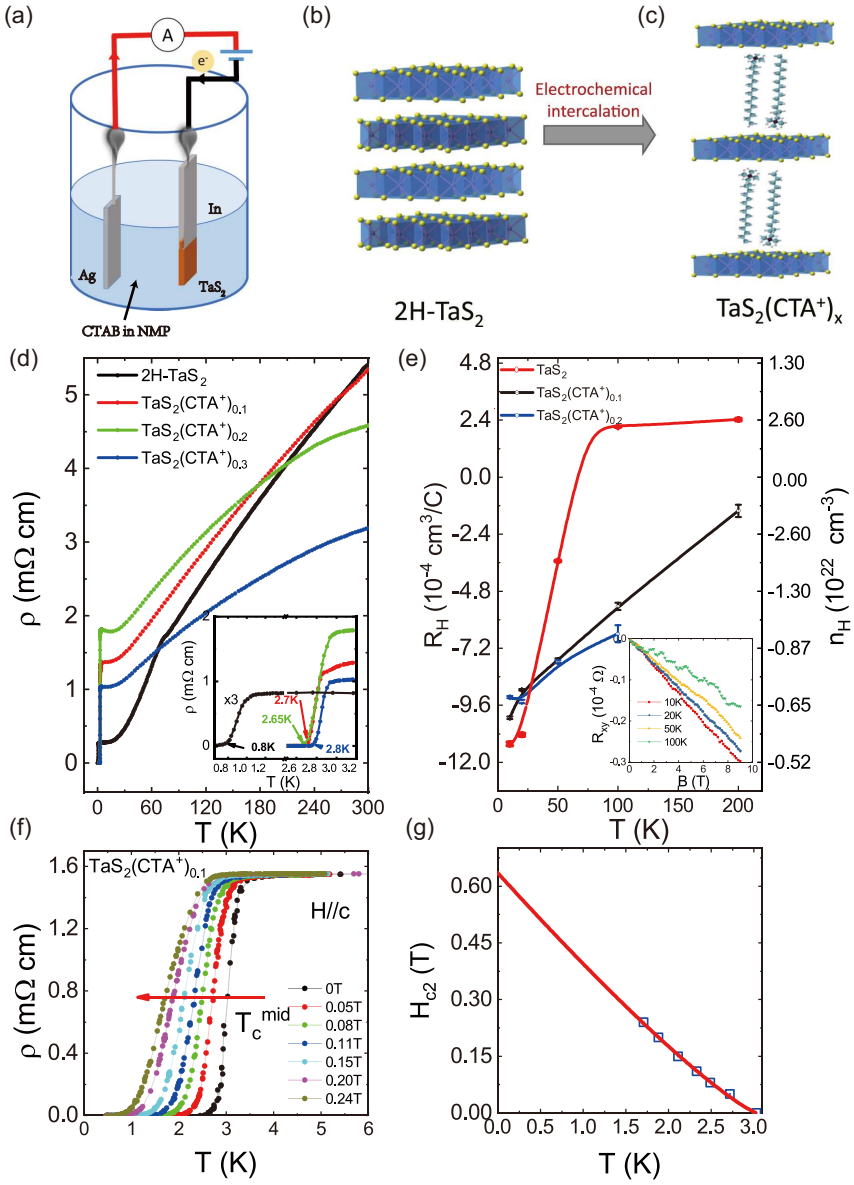

Fig. 1. (a) Schematic of the electrolytic cell; (b) and (c) crystal structures of TaS_2 and $(CTA)_xTaS_2$; (d) and (e) resistivity curve and Hall coefficient for $(CTA)_xTaS_2$; (f) resistivity curve for $(CTA)_{0.1}TaS_2$ under different magnetic fields; (g) upper critical field of $(CTA)_{0.1}TaS_2$ from the data in (f). Panel (a) is from Ref. [42], (b)–(f) are from Ref. [38].

3. Quasi-2D superconductors through organic molecule intercalation

3.1. Tunable superconductivity in TaS_2 via organic molecule intercalation

As a typical transition metal disulfide compound, the CDW and SC states in TaS_2 and the competition between them have attracted the attention of researchers.[43,44] The link between S–Ta–S covalent bonds leads to different coordination polyhedrons, and the alternating stacking of coordination polyhedrons in the *c*-axis direction brings rich isomers.[45] The most typical structures are the 1T phase and 2H phase.[46] In the 1T phase, Ta and S form octahedra; in the 2H phase, Ta and S form prisms. 1T-TaS_2 exhibits a series of CDW transitions with decreasing temperature, from incommensurate CDW at 600 K and near-commensurate CDW at 350 K to commensurate CDW at 180 K.[47] In 2H phase TaS_2, superconductivity and CDW can coexist.

In 1T-TaS_2, the CDW state can be regulated by reducing the thickness of the thin flake sample, and superconductivity can be induced through the lithium-ion-gel gating method. In 2H-TaS_2, the coexistence of CDW and SC attracts attention to investigate the completion of these different orders with the regulation of electron doping and dimensionality control. Therefore, we used electrochemical intercalation of the organic molecules to study the influence of charge doping and dimensionality reduction on the superconductivity and CDW in 2H-TaS_2.[38]

Before the intercalation of the organic molecules, the resistance curve of the bulk 2H-TaS_2 exhibits a kink near 70 K (Fig. 1(d)), and the Hall coefficient changes sign near this temperature (Fig. 1(e)), corresponding to the change in the main

carrier type and the formation of the CDW state.[48] Further lowering the temperature, the resistance curve shows superconductivity at 0.8 K, showing the coexistence of superconductivity with CDW.[49] After the intercalation of the organic molecule, the interlayer distance of 2H-TaS_2 increases from the initial 6 Å (Fig. 1(b)) to approximately 32 Å (Fig. 1(c)), which is consistent with the sum of the thickness of monolayer TaS_2 and the length of the CTA^+ molecule. This indicates that the structure of $(CTA)_xTaS_2$ is composed of one layer of TaS_2 and one layer of CTA^+ molecules with a vertical arrangement alternately stacked along the c axis. Moreover, the lattice parameter of the intercalation products in the c-axis increases slowly with increasing doping amount, which may be related to the angle change of the arrangement of organic molecules in the interlayer.[50] The TEM images of TaS_2 and $(CTA)_xTaS_2$ also confirm the structure model in Fig. 1(c).[38]

As a result, the physical properties of the intercalated products have changed greatly. In terms of electrical transport, the CDW transition near 70 K disappears after the insertion of organic molecules into TaS_2. The Hall coefficient is negative in the whole temperature range of 2–300 K, indicating that the organic molecule intercalation introduces electron doping to TaS_2 (Fig. 1(e)). At the same time, the intercalated samples show superconductivity between 2–3.5 K (Fig. 1(d)), which is much higher than that of the primitive TaS_2. This implies that the organic ions introduce carriers after intercalation, which destroys the CDW order and increases the T_c. This indicates that there may be competition between the SC and CDW orders in TaS_2. T_c is suppressed gradually with increasing applied magnetic field (Fig. 1(f)). The upper critical field shows a positive curvature (Fig. 1(g)), which confirms the type II superconductivity under the clean limit. The upper critical field obtained by fitting is 0.63 T, which is much higher than the 0.11 T of the parent TaS_2 but still lower than the Pauli limit.[51]

It has been reported that the T_c of 2H-TaS_2 can be improved from 0.5 K in the bulk sample to 2.2 K for the 3.5 nm thin flake sample.[52] The enhanced superconductivity is attributed to an enhancement of the effective electron–phonon coupling constant as the layers thin down. However, it is necessary to note that the resistivity curve of $(CTA)_{0.1}TaS_2$ in Fig. 1(f) does not resemble the features observed in quasi-2D superconductivity, although the interlayer distance of TaS_2 has been greatly increased to more than 3 nm. The increased T_c of TaS_2 is mainly attributed to the electron doping effect.

The above results show that in TaS_2 intercalated by organic molecules, the interlayer distance is increased, and the introduction of carriers inhibits the CDW order and improves the T_c. This suggests that the electrochemical organic molecule intercalation method can effectively regulate the physical properties of two-dimensional materials.

In fact, the intercalation method is a frequently used way to achieve superconductivity in TMDs due to the easy control of carrier doping. For example, the organic amine intercalated TaS_2 obtained through a solvothermal reaction achieves superconductivity, and the T_c depends on the doping level of charge transferred from the organic amine.[53] Furthermore, the liquid ammonia method is also successfully applied on T_d-WTe_2[54] and 2H-MoS_2[55] and achieves superconductivity with the intercalation of alkaline metal. However, it is difficult to obtain high-quality crystals in this way, which makes further bulk physical characterization impossible.

3.2. BKT physics in organic molecules intercalated $SnSe_2$

Apart from the improvement of the T_c in CTA^+ intercalated TaS_2, the intercalation of organic molecules into 2D materials can also induce superconductivity in an insulator. As a layered dichalcogenide compound, 1T-$SnSe_2$ is a direct band gap semiconductor with an energy gap of 1.0 eV.[56] In this material, superconductivity can be introduced through the growth of thin films,[57] ionic liquid gating[58] and Li intercalation.[59] In particular, the coexistence of superconductivity and ferromagnetism can also be observed when cobaltocene molecules are inserted into the adjacent layer of $SnSe_2$.[60] Recently, through the cointercalation of lithium and organic molecules, a close relationship between T_c and interlayer distance was reported, where T_c was independent of the content of intercalation species.[59] Finding the appropriate way to further increase the interlayer distance of $SnSe_2$ and study its transport behavior is crucial for understanding the superconducting physics of $SnSe_2$.

The interlayer distance of intercalation products can be well controlled by changing the size of organic molecules by electrochemical intercalation. Using this method, CTA^+ and TBA^+ molecules can be inserted into the interlayer of $SnSe_2$,[37] and the interlayer distances are increased from 6.12 Å (Fig. 2(a)) to 14.74 Å (Fig. 2(b)) and 18.62 Å (Fig. 2(c)), respectively. The T_c values of the corresponding products are 7.1 K and 6.4 K (Fig. 2(g)), respectively. As shown in Fig. 2(g), the phase diagram with T_c and the interlayer distance shows a dome-like behavior. Similar behavior has been observed in the intercalated HfNCl system.

Furthermore, the measurement of anisotropic susceptibility, anisotropic resistivity and BKT phase transition shows that the superconductivity after intercalation has obvious two-dimensional characteristics. On the susceptibility curve, when the magnetic field is applied in different directions, the anti-magnetic signal of the sample is tens of times different (Fig. 2(d)), indicating a strong anisotropy.

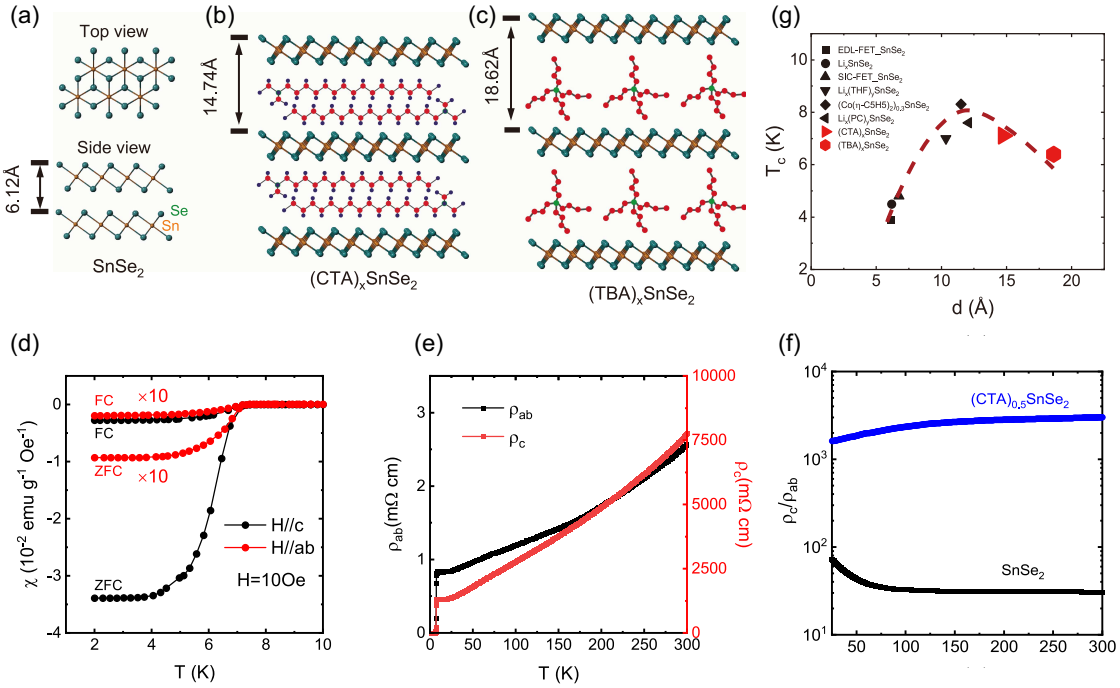

Fig. 2. (a)–(c) Crystal structures of $SnSe_2$, $(CTA)_xSnSe_2$ and $(TBA)_xSnSe_2$, respectively; (d) the magnetic susceptibility curve of $(CTA)_{0.5}SnSe_2$ with the field *H*//*c* and *H*//*ab* plane; (e) the in-plane (in black) and out-of-plane (in red) resistivity curves of $(CTA)_{0.5}SnSe_2$; (f) the temperature-dependent anisotropy resistivity ratio (ρ_c/ρ_{ab}) of $SnSe_2$ (in black) and $(CTA)_{0.5}SnSe_2$ (in blue). Panels (a)–(f) are from Ref. [37].

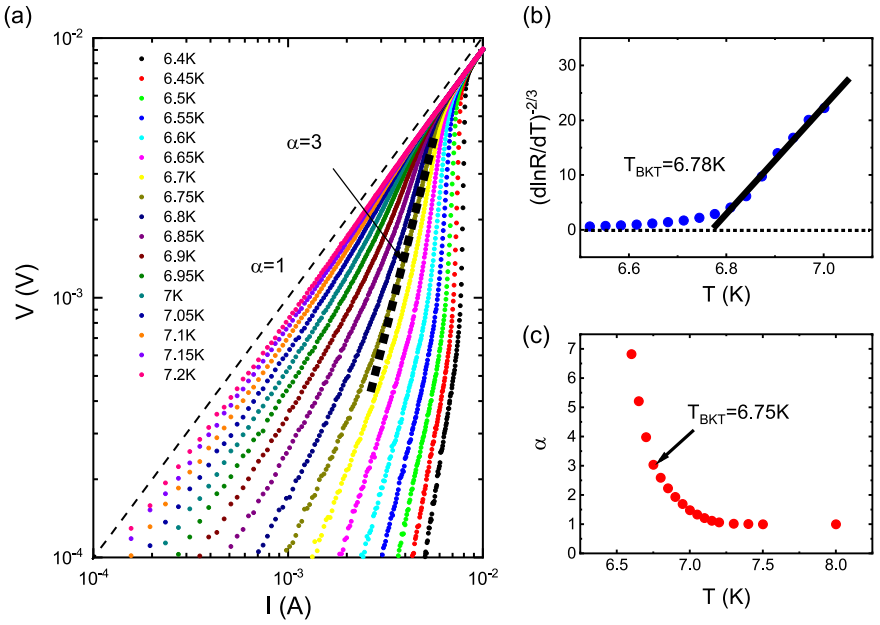

Fig. 3. (a) The *I*–*V* curves of $(CTA)_{0.5}SnSe_2$ at different temperatures around T_c; (b) the resistivity curve of $(CTA)_{0.5}SnSe_2$ with the *Y*-axis on the $[\mathrm{d}\ln R/\mathrm{d}T]^{-2/3}$ scale; (c) the temperature-dependent α obtained from (a) with the fitting function $V \propto I^{\alpha}$. Panels (a)–(c) are from Ref. [37].

On the resistivity curve, the anisotropic ratio of $(CTA)_xSnSe_2$ at 300 K is more than 2000, which is three orders of magnitude larger than the anisotropic resistivity of the parent $SnSe_2$ (Fig. 2(f)). Such enhanced anisotropy comes from the two-dimensionalization caused by organic ion intercalation. Furthermore, for two-dimensional superconductivity, the resistance curve near the superconducting transition temperature follows the Halperin–Nelson scaling law, which is expressed as $R(T) = R_0 \exp(-b/\sqrt{T - T_{\mathrm{BKT}}})$, where R_0 and b are constants.[9] The fitted BKT transition temperature is 6.78 K (Fig. 3(b)). At the same time, for the ideal two-dimensional superconducting system, due to the unbinding (or decoupling) of the vortex and anti-vortex pairs, the BKT transition occurs near the superconducting transition temperature.[61] In these BKT systems, due to the Lorentz force of the current, the vortex and anti-vortex pair will be separated, resulting in a power-law relationship between the voltage and current, i.e., $V \propto I^{\alpha}$. When α is equal to 3, the corresponding temperature is the

BKT phase transition temperature.[8] By measuring the *I*–*V* curves at different temperatures near T_c, different power-law exponents α can be obtained. When $\alpha = 3$, the corresponding BKT phase transition temperature of $(CTA)_xSnSe_2$ is 6.75 K (Fig. 3(c)), which is consistent with the BKT phase transition temperature of 6.78 K obtained by resistivity fitting. This indicates that with the insertion of organic molecules, quasi-two-dimensional superconductivity exists in $(CTA)_xSnSe_2$.

Previously, the quasi-2D SC with $T_c = 3.9$ K was observed in the ionic liquid gated 1T-$SnSe_2$ thin flake sample.[58] The intrinsic 2D superconductivity is suggested through transport measurement. The angle-dependent upper critical field of the gated thin flake 1T-$SnSe_2$ obeys the 2D Tinkham model. Furthermore, similar transport behavior is also observed in the ion-gated insulator ZrNCl, indicating the universality of such novel transport properties.[12] Our organic molecule intercalation shows an improved T_c and quasi-2D SC due to the increase of the interlayer distance in a bulk sample. These results indicate that 2D SC can also be supported in bulk samples.

3.3. Pseudogap behavior in quasi-2D high-T_c FeSe-based superconductors

Apart from the improvement of the T_c and induction of the quasi-2D SC, the intercalation of organic molecules into 2D superconductors can also favor novel transport behaviors, such as pseudogap behavior, due to the extremely improved anisotropy.

As a high-T_c iron-based superconductor with the simplest van der Waals layered structure, FeSe provides an ideal platform to study the dimensional crossover effect and underlying physics. At ambient pressure, FeSe exhibits a superconducting transition at $T_c \sim 8.5$ K.[62] By employing the electrochemical intercalation method, two new kinds of FeSe-based superconductors, namely, $(CTA)_xFeSe$ and $(TBA)_xFeSe$, with T_{c0} above 40 K, have been synthesized.[35,36] As shown in Figs. 4(a) and 4(b), the organic-ion-intercalated FeSe-based superconductors consist of alternate stacking of FeSe layers and organic molecules. With the intercalation of chemically inert organic molecules, the enhanced superconductivity and anisotropy

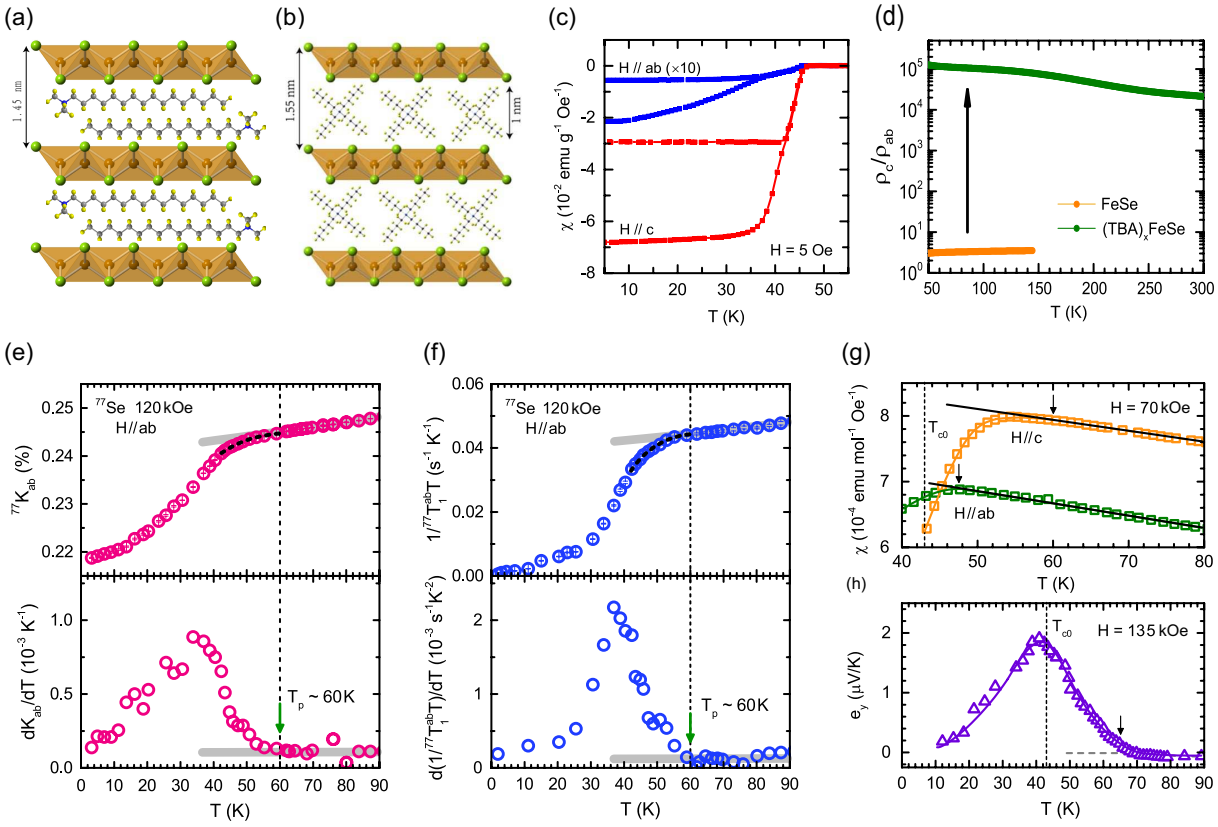

Fig. 4. (a) The schematic crystal structure of $(CTA)_xFeSe$ (cetyltrimethyl ammonium, CTA^+).[35] The distance between adjacent FeSe layers is $\sim$ 14.5 Å. (b) The schematic crystal structure of $(TBA)_xFeSe$ (tetrabutylammonium, TBA^+).[36] The distance between adjacent FeSe layers is $\sim$ 15.5 Å. (c) Temperature dependence of anisotropic magnetic susceptibility for $(TBA)_xFeSe$. An external magnetic field of 5 Oe is applied along the *ab*-plane (blue) and *c*-axis (red). (d) The anisotropy ratio of resistivity (ρ_c/ρ_{ab}) for $(TBA)_xFeSe$ and pristine FeSe. The FeSe data are adopted from Ref. [68]. (e) Temperature dependence of the Knight shift (upper panel) and its first derivative (lower panel) for $(TBA)_xFeSe$. (f) Temperature evolution of the spin-lattice relaxation rate divided by temperature (upper panel) and its first derivative (lower panel) for $(TBA)_xFeSe$. (g) The high-field magnetic susceptibility χ_{ab} and χ_c measured in field-cooling mode with a magnetic field of 7 T applied along the *ab*-plane (green) and *c*-axis (orange), respectively. The black solid lines are the extrapolation fitting curves of high-temperature behavior. The arrow indicates the onset of diamagnetism. (h) Temperature dependence of the Nernst effect under a magnetic field of 13.5 T applied along the *c*-axis. A vortex-related Nernst signal is observed well above T_{c0}. The arrow shows the onset of the vortex-related Nernst effect at $\sim$ 65 K. It should be noted that the T_p determined by the Nernst effect is slightly higher than that determined by the other probes, which suggests that the Nernst effect is more sensitive to detecting superconducting fluctuations. Panels (c)–(h) are from Ref. [63].

have been confirmed by both anisotropic magnetic susceptibility and electrical transport measurements. Taking $(TBA)_xFeSe$ as an example, as shown in Figs. 4(c) and 4(d), the significant difference in the diamagnetic shielding fraction between the two field orientations, even up to dozens of times, suggests a strong 2D character. Dramatically, the anisotropy ratio of resistivity is enhanced by approximately 5 orders of magnitude compared to bulk FeSe, supporting an intercalation-induced dimensional crossover from 3D to 2D.[63]

Nuclear magnetic resonance (NMR) is a bulk-sensitive local probe to measure electronic spin susceptibility (χ_s), which is commonly used to reveal the pseudogap behavior in high-T_c cuprate superconductors.[64,65] As shown in Figs. 4(e) and 4(f), by measuring the Knight shift and nuclear spin-lattice relaxation rate, an intrinsic pseudogap behavior below $T_p \sim 60$ K is unambiguously revealed. A weak 2D diamagnetic signal and remarkable Nernst effect far above T_{c0} further indicate the existence of strong superconducting fluctuations [Figs. 4(g) and 4(h)], confirming the preformed Cooper pairing scenario. In addition, the power-law transition with $V \sim I^{\alpha}$ in the characteristic I–V curves and the disappearance of ohmic resistance obeying the Halperin–Nelson scaling law reveal the BKT-like superconducting transition in these organic-ion-intercalated FeSe-based superconductors, definitely verifying the quasi-2D nature.

Such a result hints that the same preformed Cooper pairing scenario may be applied to FeSe/STO at the extreme 2D limit as well. The preformed pairing scenario in FeSe/STO has been clarified through *in situ* spectroscopic and electrical transport measurements.[66,67] The enhanced superconductivity and emergent pseudogap behavior reveal that dimensionality is an effective parameter to study the novel physics in iron-based superconductors. The similar pseudogap behavior observed in both cuprate superconductors and iron-based superconductors possibly suggests a crucial role of reduced dimensionality in high-T_c superconductors, especially in the emergence of pseudogap behavior.

The pseudogap behavior in organic molecule intercalated FeSe suggests that it is a powerful method to find novel transport behavior in other layered 2D superconductors.

4. Summary and prospects

Using the organic molecule intercalation method, we obtained high-quality bulk single crystals for the study of quasi-2D superconductivity and observed pseudogap behavior in the intercalated FeSe.

In recent years, thanks to the development of micro/nano processing technology, researchers have developed a new method to study quasi-2D superconductivity, which provides thin flake crystals with high crystallinity. In particular, the newly developed fieldeffect transistor using ionic liquid as the dielectric provides a clean method to tune the quasi-2D superconductivity. As a newly developed method, the organic molecule intercalation method can provide a large single crystal for further bulk measurements, which provides a new research platform for further understanding quasi-2D superconductivity.

Of course, the materials obtained by organic molecule intercalation still have some drawbacks to overcome. For example, it is still difficult to continuously control the interlayer distance and doping concentration. The intercalated samples are sensitive to air and water, and the two-dimensional materials that can be intercalated with organic molecules are limited. With the development of new methods for material preparation and modulation, the study of 2D superconductivity will gradually deepen and gradually clarify the intrinsic physical connotation between superconductivity and dimensionality.

Acknowledgements

Project supported by the Strategic Priority Research Program of the Chinese Academy of Sciences (Grant No. XDB25000000), the National Natural Science Foundation of China (Grant No. 11888101), the National Key R&D Program of China (Grant No. 2017YFA0303001), the Anhui Initiative in Quantum Information Technologies, China (Grant No. AHY160000), and the Key Research Program of Frontier Sciences, CAS (Grant No. QYZDYSSW-SLH021).

References

[1] Simonin J 1986 *Phys. Rev. B* **33** 7830
[2] Uchihashi T 2017 *Supercond. Sci. Technol.* **30** 013002
[3] Saito Y, Nojima T and Iwasa Y 2017 *Nat. Rev. Mater.* **2** 16094
[4] Hohenberg P C 1967 *Phys. Rev.* **158** 383
[5] Mermin N D and Wagner H 1966 *Phys. Rev. Lett.* **17** 1133
[6] Berezinskii V L 1971 *Sov. Phys. JETP* **32** 493
[7] Berezinskii V L 1972 *Sov. Phys. JETP* **34** 610
[8] Kosterlitz J M and Thouless D J 1973 *J. Phys. C: Solid State Phys.* **6** 1181
[9] Halperin B I and Nelson D R 1979 *J. Low. Temp. Phys.* **36** 599
[10] Reyren N, Thiel S, Caviglia A D, Kourkoutis L F, Hammerl G, Richter C, Schneider C W, Kopp T, Ruetschi A S, Jaccard D, Gabay M, Muller D A, Triscone J M and Mannhart J 2007 *Science* **317** 1196
[11] Saito Y, Nakamura Y, Bahramy M S, Kohama Y, Ye J, Kasahara Y, Nakagawa Y, Onga M, Tokunaga M, Nojima T, Yanase Y and Iwasa Y 2016 *Nat. Phys.* **12** 144
[12] Saito Y, Kasahara Y, Ye J, Iwasa Y and Nojima T 2015 *Science* **350** 409
[13] Xing Y, Zhang H M, Fu H L, Liu H, Sun Y, Peng J P, Wang F, Lin X, Ma X C, Xue Q K, Wang J and Xie X C 2015 *Science* **350** 542
[14] Qin S, Kim J, Niu Q and Shih C K 2009 *Science* **324** 1314
[15] Zhang T, Cheng P, Li W J, Sun Y J, Wang G, Zhu X G, He K, Wang L L, Ma X C, Chen X, Wang Y Y, Liu Y, Lin H Q, Jia J F and Xue Q K 2010 *Nat. Phys.* **6** 104
[16] Zhang H M, Sun Y, Li W, Peng J P, Song C L, Xing Y, Zhang Q, Guan J, Li Z, Zhao Y, Ji S, Wang L, He K, Chen X, Gu L, Ling L, Tian M, Li L, Xie X C, Liu J, Yang H, Xue Q K, Wang J and Ma X 2015 *Phys. Rev. Lett.* **114** 107003

[17] Yu Y, Ma L, Cai P, Zhong R, Ye C, Shen J, Gu G D, Chen X H and Zhang Y 2019 *Nature* **575** 156

[18] Wang Q Y, Li Z, Zhang W H, Zhang Z C, Zhang J S, Li W, Ding H, Ou Y B, Deng P, Chang K, Wen J, Song C L, He K, Jia J F, Ji S H, Wang Y Y, Wang L L, Chen X, Ma X C and Xue Q K 2012 *Chin. Phys. Lett.* **29** 037402

[19] Xing Y and Wang J 2015 *Chin. Phys. B* **24** 117404

[20] He S, He J, Zhang W, Zhao L, Liu D, Liu X, Mou D, Ou Y B, Wang Q Y, Li Z, Wang L, Peng Y, Liu Y, Chen C, Yu L, Liu G, Dong X, Zhang J, Chen C, Xu Z, Chen X, Ma X, Xue Q and Zhou X J 2013 *Nat. Mater.* **12** 605

[21] Tan S, Zhang Y, Xia M, Ye Z, Chen F, Xie X, Peng R, Xu D, Fan Q, Xu H, Jiang J, Zhang T, Lai X, Xiang T, Hu J, Xie B and Feng D 2013 *Nat. Mater.* **12** 634

[22] Zhang W H, Sun Y, Zhang J S, Li F S, Guo M H, Zhao Y F, Zhang H M, Peng J P, Xing Y, Wang H C, Fujita T, Hirata A, Li Z, Ding H, Tang C J, Wang M, Wang Q Y, He K, Ji S H, Chen X, Wang J F, Xia Z C, Li L, Wang Y Y, Wang J, Wang L L, Chen M W, Xue Q K and Ma X C 2014 *Chin. Phys. Lett.* **31** 017401

[23] Zhang W H, Li Z, Li F S, Zhang H M, Peng J P, Tang C J, Wang Q Y, He K, Chen X, Wang L L, Ma X C and Xue Q K 2014 *Phys. Rev. B* **89** 060506

[24] Li L, Wang Y Y, Komiya S, Ono S, Ando Y, Gu G D and Ong N P 2010 *Phys. Rev. B* **81** 054510

[25] Wang Y, Li L and Ong N P 2006 *Phys. Rev. B* **73** 024510

[26] Tallon J L, Storey J G and Loram J W 2011 *Phys. Rev. B* **83** 092502

[27] Corson J, Mallozzi R, Orenstein J, Eckstein J N and Bozovic I 1999 *Nature* **398** 221

[28] Jaeger H M, Haviland D B, Orr B G and Goldman A M 1989 *Phys. Rev. B* **40** 182

[29] Orr B G, Jaeger H M and Goldman A M 1985 *Phys. Rev. B* **32** 7586

[30] Guo Y, Zhang Y F, Bao X Y, Han T Z, Tang Z, Zhang L X, Zhu W G, Wang E G, Niu Q, Qiu Z Q, Jia J F, Zhao Z X and Xue Q K 2004 *Science* **306** 1915

[31] Eom D, Qin S, Chou M Y and Shih C K 2006 *Phys. Rev. Lett.* **96** 027005

[32] Staley N E, Wu J, Eklund P, Liu Y, Li L and Xu Z 2009 *Phys. Rev. B* **80** 184505

[33] Cao Y, Mishchenko A, Yu G L, Khestanova E, Rooney A P, Prestat E, Kretinin A V, Blake P, Shalom M B, Woods C, Chapman J, Balakrishnan G, Grigorieva I V, Novoselov K S, Piot B A, Potemski M, Watanabe K, Taniguchi T, Haigh S J, Geim A K and Gorbachev R V 2015 *Nano Lett.* **15** 4914

[34] Xi X, Zhao L, Wang Z, Berger H, Forro L, Shan J and Mak K F 2015 *Nat. Nanotechnol.* **10** 765

[35] Shi M Z, Wang N Z, Lei B, Shang C, Meng F B, Ma L K, Zhang F X, Kuang D Z and Chen X H 2018 *Phys. Rev. Mater.* **2** 074801

[36] Shi M Z, Wang N Z, Lei B, Ying J J, Zhu C S, Sun Z L, Cui J H, Meng F B, Hang C S, Ma L K and Chen X H 2018 *New J. Phys.* **20** 123007

[37] Ma L K, Shi M Z, Kang B L, Peng K L, Meng F B, Zhu C S, Cui J H, Sun Z L, Wang H H, Lei B, Wu T and Chen X H 2020 *Phys. Rev. Mater.* **4** 124803

[38] Wang N Z, Shi M Z, Shang C, Meng F B, Ma L K, Luo X G and Chen X H 2018 *New J. Phys.* **20** 023014

[39] Che G C, Du Y K, Dong C, Wu F and Zhao Z X 1995 *J. Mater. Res.* **10** 1358

[40] Yu Y, Yang F, Lu X F, Yan Y J, Cho Y H, Ma L, Niu X, Kim S, Son Y W, Feng D, Li S, Cheong S W, Chen X H and Zhang Y 2015 *Nat. Nanotechnol.* **10** 270

[41] Xi X X, Wang Z F, Zhao W W, Park J H, Law K T, Berger H, Forro L, Shan J and Mak K F 2016 *Nat. Phys.* **12** 139

[42] Shi M Z, Kang B L, Meng F B, Wu T and Chen X H 2022 *Acta Phys. Sin.* **71** 127403 (in Chinese)

[43] Ang R, Tanaka Y, Ieki E, Nakayama K, Sato T, Li L J, Lu W J, Sun Y P and Takahashi T 2012 *Phys. Rev. Lett.* **109** 176403

[44] Ang R, Miyata Y, Ieki E, Nakayama K, Sato T, Liu Y, Lu W J, Sun Y P and Takahashi T 2013 *Phys. Rev. B* **88** 115145

[45] Friend R H and Yoffe A D 1987 *Adv. Phys.* **36** 1

[46] Qian X, Liu J, Fu L and Li J 2014 *Science* **346** 1344

[47] Sipos B, Kusmartseva A F, Akrap A, Berger H, Forro L and Tutis E 2008 *Nat. Mater.* **7** 960

[48] Naito M and Tanaka S 1982 *J. Phys. Soc. Jpn.* **51** 219

[49] Nagata S, Aochi T, Abe T, Ebisu S, Hagino T, Seki Y and Tsutsumi K 1992 *J. Phys. Chem. Solids* **53** 1259

[50] Akat H, Tasdelen M A, Du Prez F and Yagci Y 2008 *Eur. Polym. J.* **44** 1949

[51] Vicent J L, Hillenius S J and Coleman R V 1980 *Phys. Rev. Lett.* **44** 892

[52] Navarro-Moratalla E, Island J O, Manas-Valero S, Pinilla-Cienfuegos E, Castellanos-Gomez A, Quereda J, Rubio-Bollinger G, Chirolli L, Angel Silva-Guillen J, Agrait N, Steele G A, Guinea F, van der Zant H S J and Coronado E 2016 *Nat. Commun.* **7** 11043

[53] Gamble F R, Osiecki J H, Cais M and Pisharody R 1971 *Science* **174** 493

[54] Zhu L, Li Q Y, Lv Y Y, Li S, Zhu X Y, Jia Z Y, Chen Y B, Wen J and Li S C 2018 *Nano Lett.* **18** 6585

[55] Somoano R B and Rembaum A 1971 *Phys. Rev. Lett.* **27** 402

[56] Bhatt V P, Gireesan K and Pandya G R 1989 *J. Cryst. Growth* **96** 649

[57] Zhang Y M, Fan J Q, Wang W L, Zhang D, Wang L L, Li W, He K, Song C L, Ma X C and Xue Q K 2018 *Phys. Rev. B* **98** 220508

[58] Zeng J, Liu E, Fu Y, Chen Z, Pan C, Wang C, Wang M, Wang Y, Xu K, Cai S, Yan X, Wang Y, Liu X, Wang P, Liang S J, Cui Y, Hwang H Y, Yuan H and Miao F 2018 *Nano Lett.* **18** 1410

[59] Wu H L, Li S, Susner M, Kwon S, Kim M, Haugan T and Lv B 2019 *2D Mater.* **6** 045048

[60] Li Z, Zhao Y, Mu K, Shan H, Guo Y, Wu J, Su Y, Wu Q, Sun Z, Zhao A, Cui X, Wu C and Xie Y 2017 *J. Am. Chem. Soc.* **139** 16398

[61] Beasley M R, Mooij J E and Orlando T P 1979 *Phys. Rev. Lett.* **42** 1165

[62] Williams A J, McQueen T M and Cava R J 2009 *Solid State Commun.* **149** 1507

[63] Kang B L, Shi M Z, Li S J, Wang H H, Zhang Q, Zhao D, Li J, Song D W, Zheng L X, Nie L P, Wu T and Chen X H 2020 *Phys. Rev. Lett.* **125** 097003

[64] Warren W W, Jr., Walstedt R E, Brennert G F, Cava R J, Tycko R, Bell R F and Dabbagh G 1989 *Phys. Rev. Lett.* **62** 1193

[65] Berthier C, Julien M H, Horvatic M and Berthier Y 1996 *J. Phys. I France* **6** 2205

[66] Xu Y, Rong H, Wang Q, Wu D, Hu Y, Cai Y, Gao Q, Yan H, Li C, Yin C, Chen H, Huang J, Zhu Z, Huang Y, Liu G, Xu Z, Zhao L and Zhou X J 2021 *Nat. Commun.* **12** 2840

[67] Faeth B D, Yang S L, Kawasaki J K, Nelson J N, Mishra P, Parzyck C T, Li C, Schlom D G and Shen K M 2021 *Phys. Rev. X* **11** 021054

[68] Vedeneev S I, Piot B A, Maude D K and Sadakov A V 2013 *Phys. Rev. B* **87** 134512